

## REVIEW

## Interactions of organotin with biological systems

M Teresa Musmeci, Grazia Madonia, M Teresa Lo Giudice, Arturo Silvestri, Giuseppe Ruisi and Renato Barbieri\*

Institute of Histology and Embryology, and Department of Inorganic Chemistry, University of Palermo, Via Archirafi 26–28, Palermo 90123, Italy

The bonding and structure in the environments of tin atoms in organotin–biological molecules has been investigated by  $^{119}\text{Sn}$  Mössbauer spectroscopy, mainly through the rationalization of the nuclear quadrupole splitting parameter by point-charge model approaches.

Organotin moieties  $\text{R}_2\text{Sn}^{\text{IV}}$  and  $\text{R}_3\text{Sn}^{\text{IV}}$  ( $\text{R} = \text{Me}$ ,  $\text{nBu}$ ,  $\text{Ph}$ ) generally assume trigonal-bipyramidal type configurations in membranes of human erythrocytes, when incubated with whole erythrocytes and erythrocyte ghosts at the level of micromolar ( $\mu\text{mol dm}^{-3}$ ) organotin per mg of membrane protein. Corresponding structures are assumed by  $\text{Me}_2\text{Sn}^{\text{IV}}$  and  $\text{Me}_3\text{Sn}^{\text{IV}}$  in the cytoplasm. Ethanolic  $\text{Me}_2\text{SnCl}_2$  yielded distorted *trans*-octahedral species when reacted with ghost cells. These configurations may in principle originate through coordination of the metal by donor nitrogen or oxygen atoms from the cell constituents, such as protein side chains and related component molecules, carbohydrate fragments, and phospholipids, according to data from various model systems. Hydrolyzed species, such as bis(chlorodiorganotin) oxides and triorganotin hydroxides, could also occur for the *n*-butyltin and phenyltin species.

The moieties  $\text{Me}_2\text{Sn}^{\text{IV}}$  and  $\text{Alk}_3\text{Sn}^{\text{IV}}$  ( $\text{Alk} = \text{Me}$ ,  $\text{Et}$ ,  $\text{nBu}$ ), present as the hydrolysis products  $\text{Me}_2\text{Sn}(\text{OH})_2$  and  $\text{Alk}_3\text{SnOH}$  at physiological pH in the aqueous phase (eventually coordinated by donor atoms from buffers), react with thiol groups of model molecules, as well as of feline and rat hemoglobin, forming tetrahedral or trigonal-bipyramidal tin sites characterized by covalent  $\text{Sn}–\text{S}$  bonds ( $\text{C}_2\text{SnS}$ ,  $\text{C}_2\text{SnS}_2$  and  $\text{C}_3\text{SnS}$  skeletons); tin atoms are eventually further coordinated by nitrogen donors from amino acid fragments or from buffers, as well as by hydroxyl oxygen.

**Keywords:** Organotin, biological molecules, Mössbauer

\* Authors to whom correspondence should be addressed.

## INTRODUCTION

Organotin(IV) compounds are known to interact with cell membranes and with proteins. The moieties  $\text{nBu}_3\text{Sn}^{\text{IV}}$  form spheres connected to the membranes of human erythrocytes,<sup>1,2</sup> possibly consisting of micelles, with the organic radicals interacting with the lipid bilayer. The formation of organotin(IV) micelles has been reported recently.<sup>3</sup>

The neutral species  $\text{R}_3\text{SnX}$  ( $\text{X} = \text{Cl}$ ,  $\text{OH}$ ;  $\text{R} = \text{Me}$ ,  $\text{Et}$ ,  $\text{nPr}$ ,  $\text{nBu}$ ,  $\text{Ph}$ ) occur in membranes of rat liver mitochondria, of human and ox erythrocytes, as well as in liposomes of lecithin and of bacterial phosphatidylethanolamine.<sup>4–7</sup> The  $\text{nBu}_3\text{SnX}$  derivatives are the most efficient in promoting  $\text{Cl}^-/\text{OH}^-$  anion exchange through the membrane, which is connected to the lipophilicity of the  $\text{nBu}$  radicals and to the consequent intercalation of  $\text{nBu}_3\text{SnX}$  into the lipid bilayer.<sup>6,7</sup>

The moieties  $\text{R}_n\text{Sn}^{\text{IV}}$  ( $n = 2$  and  $3$ ) bind to proteins and glycoproteins of cell membranes, as well as to cellular proteins: for example, (i)  $\text{Et}_3\text{Sn}^{\text{IV}}$  to ATPase and hexokinase of trout, feline and human erythrocytes;<sup>8</sup> (ii)  $\text{nBu}_2\text{Sn}^{\text{IV}}$  and  $\text{nBu}_3\text{Sn}^{\text{IV}}$  to band 3 proteins (e.g.  $\text{Na}^+$ ,  $\text{K}^+$ -ATPase, acetylcholine esterase) of human erythrocyte membrane;<sup>9</sup>  $\text{nBu}_2\text{Sn}^{\text{IV}}$  interacts also with proteins of band 7 and 9,<sup>9</sup> and binding to skeletal muscle membranes occurs;<sup>9</sup> (iii)  $\text{nBu}_3\text{Sn}^{\text{IV}}$  to plasma membranes and cellular proteins of murine erythroleukemic cells, inducing denaturations;<sup>10</sup> (iv)  $\text{Et}_3\text{Sn}^{\text{IV}}$  and  $\text{Ph}_3\text{Sn}^{\text{IV}}$  to the proteolipid fraction from membranes of rat liver mitochondria;  $\text{Et}_3\text{Sn}^{\text{IV}}$  to ATPase, and  $\text{Ph}_3\text{Sn}^{\text{IV}}$  to proteins with mass 5000–6000.<sup>11,12</sup>

The moieties  $\text{R}_3\text{Sn}^{\text{IV}}$  show weak Coulomb interaction with the phosphodiester group of phospholipids: for example, (i)  $\text{Et}_3\text{Sn}^{\text{IV}}$  with phospholipids from membranes of rat liver mitochondria;<sup>13</sup> (ii)  $\text{Me}_3\text{Sn}^{\text{IV}}$  and  $\text{Bu}_3\text{Sn}^{\text{IV}}$  with phos-

phatidylcholine liposomes.<sup>14</sup>

Feline and rat hemoglobin form complexes with  $R_3Sn^{IV}$  and  $Me_2Sn^{IV}$ .<sup>15–19</sup> Species such as  $(Et_3Sn)_2$  (hemoglobin tetramer) are formed, characterized by high affinity between tin and hemoglobin.<sup>15, 16</sup> The moiety  $Et_3Sn^{IV}$  is linked to the  $\alpha$ -subunits of the tetramer, through the thiol sulfur from cysteine-13 and the imidazole nitrogen of histidine-113, axially coordinating into a trigonal-bipyramidal type structure.<sup>20</sup> Analogous bonding situations would occur for  $Me_3Sn^{IV}$ - and  $nBu_3Sn^{IV}$ -hemoglobin.<sup>17</sup> Facial  $SnC_3$  fragments, as well as bonding by two imidazole nitrogen atoms, have been also assumed.<sup>15, 21</sup>  $Me_2Sn^{IV}$  would be involved in tetrahedral, as well as trigonal-bipyramidal, complexes with 'hemoglobin phases'<sup>18, 19</sup> (*vide infra*).

It seems worthy of note that the structural assumptions reported above are generally based on the interpretation of experimental data reflecting bonding and coordination geometries, but are, on the other hand, rather speculative in some other instances. Moreover, information is sometimes missing about the nature of the solutions of organotin compounds employed in the experiments, and the addition of solid organotins to biological systems might have occurred. In addition, organotin hydrolysis processes are often ignored. These circumstances, in conjunction with the different experimental conditions and procedures employed in the individual studies, may originate incongruities and differing interpretations as reported above.

The work reported in the present paper concerns molecular aspects of the *in vitro* interaction of organotin compounds with erythrocytes (representative of simple biological cells and their membranes), as well as with hemoglobin (a model protein). Organotin–native DNA systems<sup>22–26</sup> are discussed in a following paper. Structure and bonding environments of the tin atoms were investigated by  $^{119}Sn$  Mössbauer spectroscopy, selected as a technique which allows the study of the coordination sphere of a metal irrespective of the molecular complexity of the medium.

## EXPERIMENTAL

### Organotin–human erythrocyte systems<sup>27</sup>

Erythrocytes were isolated by centrifugation from human blood (obtained from blood banks), washed separately with PBS ( $NaH_2PO_4$  +

$Na_2HPO_4$ , 5 mmol  $dm^{-3}$ , NaCl 0.15 mol  $dm^{-3}$ , pH 8.0), and pelleted by centrifuging at 2500 rpm for 15 min. Pellets (3–8  $cm^3$ ) were added with  $R_nSnCl_{4-n}$  ( $R$  = alkyl) (1 mol  $dm^{-3}$  in  $C_2H_5OH$ ) as well as with aqueous  $Me_2Sn(OH)_2$  and  $Me_3SnOH$  (each 10–20 mmol  $dm^{-3}$ ) (final organotin concentration = 5–10 mmol  $dm^{-3}$ ;  $C_2H_5OH$  = 1%), and incubated at 37 °C for 15 min. After washing with PBS, 2  $cm^3$  of the organotin–erythrocyte suspension was frozen in liquid nitrogen and submitted to Mössbauer spectroscopy, by procedures described elsewhere.<sup>18, 27</sup> A further fraction of the erythrocyte–organotin pellets (*vide supra*) was hemolyzed with 5P8 ( $Na_2HPO_4$  +  $NaH_2PO_4$ , 5 mmol  $dm^{-3}$ , pH 8). The ghost cells were washed with PBS and centrifuged and the supernatant was dried by lyophilization, both being eventually submitted to Mössbauer spectroscopy. The interaction of organotins with erythrocyte membranes was effected by preparing ghost cells through hemolysis of erythrocytes with 5P8 (*vide supra*), and adding organotins in ethanol or aqueous solutions, followed by incubation and centrifugation, with procedures and conditions analogous to those described above.

### Organotin–rat hemoglobin complexes<sup>17–19</sup>

Rat erythrocytes were hemolyzed as above, and the concentration of hemoglobin was determined by visible spectrophotometry. The  $Me_2Sn^{IV}$  and  $R_3Sn^{IV}$  derivatives (5–7  $\mu$ mol, from aqueous stock solutions containing 5–10 mmol  $dm^{-3}$  in

**Table 1** The tin environment in organotins as a function of the  $^{119}Sn$  Mössbauer parameter nuclear quadrupole splitting ( $\Delta E$ )<sup>a</sup>

Species <sup>b</sup>	Structure <sup>c</sup>	$\Delta E$ range <sup>d</sup> (mm $s^{-1}$ )
$R_nSnA_{4-n}$	tet	0.00–2.80
$R_2SnA_4$	oct; <i>cis</i> - $R_2$	1.63–2.34
$Alk_2SnA_3$	tbp; equatorial Alk	2.85–3.12
$Alk_2SnA_4$	oct; <i>trans</i> -Alk <sub>2</sub>	3.64–4.75
$Ph_2SnA_3$	tbp; equatorial Ph	2.40–3.05
$Ph_2SnA_4$	oct; <i>trans</i> -Ph <sub>2</sub>	3.35–4.30
$Alk_3SnA_2$	tbp; equatorial Alk	3.18–4.57
$Ph_3SnA_2$	tbp; equatorial Ph	2.73–4.00

<sup>a</sup>A collection of literature data<sup>28, 31, 32</sup> for the fingerprint assignment of most common geometries.

<sup>b</sup> $R$  = Alk, Ph;  $n$  = 1–3; A = ligand donor atom other than C.

<sup>c</sup>Abbreviations: tet = tetrahedral; oct = octahedral; tbp = trigonal-bipyramidal.

<sup>d</sup>Experimental data.

0.2 mol dm<sup>-3</sup> Hepes buffer, pH 7.4, for R = Me, Et, as well as from stock 0.1 mol dm<sup>-3</sup> nBu<sub>3</sub>SnCl in ethanol) were respectively added to 3.5–4.5 μmol of hemoglobin (the final volume being 5–6 cm<sup>3</sup>) and the solution was left to crystallize at 4 °C overnight. The interaction of organotins with crystalline rat hemoglobin was effected by preparing solid samples of hemoglobin (3.5 μmol in 5 cm<sup>3</sup> of H<sub>2</sub>O added to 0.5 cm<sup>3</sup> of 0.2 mol dm<sup>-3</sup> Hepes buffers at pH 7.4, and crystallized on standing at 4 °C for one day), which were suspended in H<sub>2</sub>O, added with 7 μmol of the organotin compound, stirred, and stored overnight at 4 °C.

### Mössbauer Spectroscopy, and fingerprint and point-charge model treatment of the nuclear quadrupole splitting parameter $\Delta E$ , for structural attribution

The apparatus and procedures employed in the determination of <sup>119</sup>Sn Mössbauer spectra were as reported earlier.<sup>17, 18, 25</sup>

The geometry of the environment of the tin atoms was first estimated from the experimental parameters  $\Delta E$  by fingerprint assignments, e.g. according to the data in Table 1. Detailed information on structure and bonding has been subsequently extracted from calculations of  $\Delta E$  obtained by the following procedures:

- (I) The literal version of the point-charge model (generally concerned with regular structures), where the contributions of *all* (assumed) valence electron pairs to the magnitude of the electric field gradient tensor at the tin nucleus have been taken into account in the calculations.<sup>28</sup>
- (II) The point-charge model approach accounting *only* for Sn–C valence electrons in dictating the magnitude of the electric field gradient, with the contributions of bonds between tin and electronegative ligand atoms (Sn–A) being ignored.<sup>29, 30</sup>

Calculations according to (I) and (II) have been effected employing partial nuclear quadrupole splitting parameters (p.q.s.) taken from the literature.<sup>18, 28, 30–32</sup> Model (II) allows the correlation of  $\Delta E_{\text{exp, calcd}}$  data with distortions from ideal octahedral, trigonal-bipyramidal and tetrahedral structures, and estimates of the order of magnitude of C–Sn–C angles in R<sub>2</sub>SnA<sub>3, 4</sub>, and C–Sn–A angles in R<sub>3</sub>SnA<sub>1, 2</sub>.<sup>29, 30</sup>

## RESULTS AND DISCUSSION

### The nature of the reagent organotin species and of the hydrolysis products

Ethanolic solutions of organotins [R<sub>2</sub>SnCl<sub>2</sub>·(C<sub>2</sub>H<sub>5</sub>OH)<sub>2</sub> and R<sub>3</sub>SnCl(C<sub>2</sub>H<sub>5</sub>OH)] show quasi-regular *trans*-R<sub>2</sub> octahedral and trigonal-bipyramidal (equatorial C atoms) configurations respectively, as extracted from experimental  $\Delta E$  data [Table 2(A)] and point-charge model (II) calculations<sup>26</sup> (see the Experimental section.) Aqueous methyltins (at pH around 4) consist of trigonal-bipyramidal species, [Me<sub>2</sub>Sn(OH)·(OH<sub>2</sub>)<sub>n</sub>]<sup>+</sup> and [Me<sub>3</sub>Sn(OH<sub>2</sub>)<sub>2</sub>]<sup>+</sup> [Table 2(B)] with equatorial carbon and hydroxyl oxygen atoms, according to point-charge model (I) estimates.<sup>17, 26</sup> The hydroxides in aqueous media [Table 2(B)] and their adducts with ligand molecules, such as excess Hepes buffer, are generally trigonal-bipyramidal too, except Me<sub>2</sub>Sn(OH)<sub>2</sub> which is tetrahedral.<sup>17, 18</sup>

As reported in the Experimental section, the organotin–human erythrocytes, –erythrocyte ghosts, and –rat hemoglobin systems (as well as related models, *vide infra*) were obtained essentially from aqueous media, eventually buffered at neutral pH.<sup>17–19, 27, 33</sup> Water-insoluble hydrolyzed organotin derivatives may then form, together with, or in place of, organotins bound to component molecules of biological systems, whose Mössbauer parameters are listed in Table 2(C). Oxides (R<sub>2</sub>SnO)<sub>n</sub> and stannoxanes (R<sub>3</sub>Sn)<sub>2</sub>O are tetrahedral solid-state species;<sup>38–41</sup> bis(chlorodiorganotin) oxides (R<sub>2</sub>SnCl)<sub>2</sub>O are trigonal-bipyramidal ladder- or staircase-type polymers,<sup>36, 42–45</sup> and hydroxides (R<sub>3</sub>SnOH) are quasi-regular trigonal-bipyramidal polymeric species with axially bridging OH groups.<sup>46, 47</sup> Structure and bonding in these molecules, as inferred from Mössbauer parameters and the related point-charge model treatments, often agree remarkably with the correct crystallographic data; this is shown in Fig. 1 for (R<sub>2</sub>SnCl)<sub>2</sub>O species, which are likely to occur in our systems (*vide infra*).

### Organotin–erythrocytes and –erythrocyte membranes

The Mössbauer parameters of these systems<sup>27</sup> are summarized in Table 3. The magnitude of the isomer shift ( $\delta$ ) data corresponds to values reported for the individual R<sub>n</sub>Sn<sup>IV</sup> moieties.<sup>28–32, 34</sup>

**Table 2**  $^{119}\text{Sn}$  Mössbauer parameters of organotin species interacted with human erythrocytes and erythrocyte ghosts, with rat hemoglobin, and with calf thymus DNA (see Ref. 26), and the parameters of eventual hydrolysis products<sup>a</sup>

Compound or system <sup>b</sup>	$\delta$ (mm s <sup>-1</sup> ) <sup>c</sup>	$\Delta E$ (mm s <sup>-1</sup> ) <sup>d</sup>	Ref.
(A) Ethanol solutions <sup>e</sup>			
$\text{Alk}_2\text{SnCl}_2(\text{C}_2\text{H}_5\text{OH})_2^f$	1.35–1.59	3.85–4.05	25, 26
$\text{Ph}_2\text{SnCl}_2(\text{C}_2\text{H}_5\text{OH})_2$	1.31	3.58	26
$\text{Alk}_3\text{SnCl}(\text{C}_2\text{H}_5\text{OH})^f$	1.33–1.48	3.31–3.43	26, 17
$\text{Ph}_3\text{SnCl}(\text{C}_2\text{H}_5\text{OH})$	1.29	3.07	26
(B) Aqueous solutions <sup>e</sup>			
$[\text{Me}_2\text{Sn}(\text{OH})(\text{OH}_2)_n]^+$	1.20	3.04	25, 26
$\text{Me}_2\text{Sn}(\text{OH})_2$	0.94	2.24	18
$\text{Me}_2\text{Sn}(\text{OH})_2 \cdot \text{Hepes}$	1.11	3.03	18
$[\text{Me}_3\text{Sn}(\text{OH}_2)_2]^+$	1.50	3.87	17
$\text{Me}_3\text{Sn}(\text{OH})(\text{OH}_2)$	1.24	2.80	17
$\text{Me}_3\text{Sn}(\text{OH}) \cdot \text{Hepes}$	1.34	3.31	17
$\text{Et}_3\text{Sn}(\text{OH})(\text{OH}_2)$	1.30; 1.33	2.98; 3.02	17, 26
$\text{Et}_3\text{Sn}(\text{OH}) \cdot \text{Hepes}$	1.45	3.41	17
(C) Solids <sup>g</sup>			
$(\text{Me}_2\text{SnO})_n$	0.91–1.00	1.82–2.07	34, 35
$(\text{Et}_2\text{SnO})_n$	1.01–1.05	2.10–2.33	34, 26
$(\text{Et}_2\text{SnCl})_2\text{O}$	1.34; 1.50	3.34; 3.41	34, 36
$(\text{nBu}_2\text{SnO})_n$	0.94–1.15	1.95–2.20	34
$(\text{nBu}_2\text{SnCl})_2\text{O}$	1.25–1.46	3.20–3.26	34, 36
$(\text{nOct}_2\text{SnO})_n$	0.96–1.03	2.00–2.05	34
$(\text{nOct}_2\text{SnCl})_2\text{O}$	1.42	3.26	26
$(\text{Ph}_2\text{SnO})_n$	0.89–0.95	1.73–2.00	34
$(\text{Ph}_2\text{SnCl})_2\text{O}$	1.26	3.08	36
$(\text{nBu}_3\text{Sn})_2\text{O}$	1.10–1.29	1.15–2.40	34, 37
$\text{nBu}_3\text{SnOH}$	1.37–1.46	2.99–3.24	34, 37
$(\text{nOct}_3\text{Sn})_2\text{O}^h$	1.21	1.57	37
$\text{nOct}_3\text{SnOH}^h$	1.35	2.95	37
$(\text{Ph}_3\text{Sn})_2\text{O}$	1.07; 1.08	1.63; 2.15	37, 34
$\text{Ph}_3\text{SnOH}$	1.16–1.35	2.68–2.83	34, 37

<sup>a</sup> Measured at liquid-nitrogen temperature.

<sup>b</sup> Hepes is *N*-2-hydroxyethylpiperazine-*N'*-2-ethanesulfonic acid; buffer, pH = 7.40.  $[\text{Me}_2\text{Sn}(\text{OH})(\text{OH}_2)_n]^+$  and  $[\text{Me}_3\text{Sn}(\text{OH}_2)_2]^+$  occur at pH  $\approx$  4.0, and the hydroxides at pH > 7.0.<sup>26</sup>

<sup>c</sup> Isomer shift with respect to room-temperature  $\text{CaSnO}_3$ ; individual values or ranges of values.

<sup>d</sup> Nuclear quadrupole splitting; individual values or ranges of values.

<sup>e</sup> Glassy absorbers, frozen by immersion into liquid nitrogen.<sup>18</sup> Solutions (A) are 0.1 mol dm<sup>-3</sup>, and (B) are 5–20 mmol dm<sup>-3</sup>.

<sup>f</sup> Alk = Me, Et, nBu, nOct.

<sup>g</sup> Unless otherwise stated.

<sup>h</sup> Oil.

The  $\Delta E$  data for systems 1, 2 and 4–9 clearly indicate the occurrence of trigonal-bipyramidal species, whilst system 3 would assume a *trans*-octahedral structure, according to  $\Delta E$  ranges for fingerprint assignments reported in Table 1. The

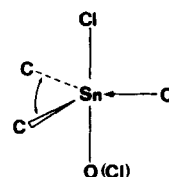


**Figure 1** The nature of the environment of tin atoms in bis(chlorodiorganotin) oxides. C–Sn–C angles in  $\{[\text{Me}_2\text{Sn}(\text{NCS})_2\text{O}]_2\}$ ,  $\{(\text{Me}_2\text{SnCl})_2\text{O}\}_2$ ,  $\{(\text{Ph}_2\text{SnCl})_2\text{O}\}_2$ , and related species, are in the range 122–141°, as determined by X-ray diffractometry.<sup>36, 42–45</sup> Point-charge model (II) estimates (see the Experimental section of this paper) are as follows [from  $\Delta E_{\text{exp}}$  data in Table 2(C)]:  $(\text{Alk}_2\text{SnCl})_2\text{O}$ , C–Sn–C = 125–131°;  $(\text{Ph}_2\text{SnCl})_2\text{O}$ , C–Sn–C = 135°.

possible geometries of the environments of the tin atoms are reported in Fig. 2, in conjunction with distortions, as estimated by point-charge model calculations.<sup>27</sup>

The molecular nature of the products 1–9, Table 3, is subsequently explored in connection with compounds formed through hydrolytic processes, as well as with organotin–model complexes and/or methyltin–ligands species formed in aqueous solutions.

The occurrence, or the formation, of tetrahedral or quasi-tetrahedral hydrolysis products, such as the water-soluble species  $\text{Me}_2\text{Sn}(\text{OH})_2$  and  $\text{Me}_3\text{Sn}(\text{OH})(\text{OH}_2)$ , and the solids  $(\text{R}_2\text{SnO})_n$  and  $(\text{R}_3\text{Sn})_2\text{O}$  (*vide supra*, Table 2(B) and (C)) may be safely excluded by inspection of the  $\Delta E$  data in Tables 2 and 3; instead, the trigonal-bipyramidal (solid-state) species  $(\text{R}_2\text{SnCl})_2\text{O}$  and  $\text{R}_3\text{SnOH}$  (R = nBu and Ph) could be present in the systems 6, 8, and 7, 9, respectively (Tables 2 and 3; Figs. 1 and 2).

The biological molecules providing ligand atoms to tin in the systems 1–9, Table 3 and Fig. 2, could be assumed according to the following (oversimplified) scheme.

- (i) In proteins, peptides and amino acids from erythrocyte membranes and cytoplasm, oxygen atoms donate from carboxyl, carbonyl and hydroxide; amino and heterocyclic nitrogen atoms, and thiol sulfur, also donate.
- (ii) In oligosaccharides from glycolipids and glycoproteins, alcoholic hydroxyls donate.
- (iii) In phospholipids in the lipid bilayers, oxygen atoms of phosphodiester groups donate.

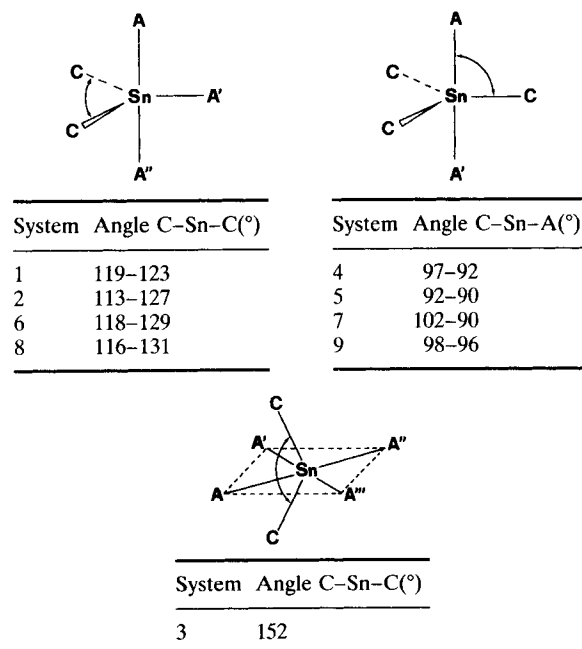
These hypotheses are tested here by taking into account the Mössbauer parameters, as well as representative values of bond angles from

**Table 3**  $^{119}\text{Sn}$  Mössbauer parameters of organotin(IV)–human erythrocyte systems<sup>a</sup>

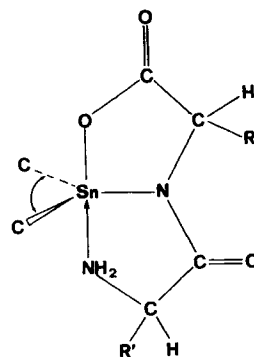
System no.	Reacted organotins, and systems <sup>b</sup>	$\delta$ (mm s <sup>-1</sup> ) <sup>c</sup>	$\Delta E$ (mm s <sup>-1</sup> ) <sup>c</sup>	$\Gamma_1, \Gamma_2$ (mm s <sup>-1</sup> ) <sup>d</sup>
1	$\text{Me}_2\text{Sn}(\text{OH})_2$ –whole erythrocytes, –cytoplasm, and –ghost cells	1.09–1.22	2.96–3.13	0.85–1.27
2	$\text{Me}_2\text{SnCl}_2(\text{C}_2\text{H}_5\text{OH})_2$ –whole erythrocytes, and –membranes	1.15–1.32	2.75–3.24	0.84–1.85
3	$\text{Me}_2\text{SnCl}_2(\text{C}_2\text{H}_5\text{OH})_2$ –ghost cells	1.23	3.77	0.90–1.13
4	$\text{Me}_3\text{SnOH}(\text{OH}_2)$ –whole erythrocytes, –cytoplasm, and –ghost cells	1.28–1.35	3.20–3.37	0.64–1.10
5	$\text{Me}_3\text{SnCl}(\text{C}_2\text{H}_5\text{OH})_2$ –whole erythrocytes, and –ghost cells	1.23–1.35	3.37–3.48	0.73–1.14
6	$\text{nBu}_2\text{SnCl}_2(\text{C}_2\text{H}_5\text{OH})_2$ –whole erythrocytes, –membranes, and –ghost cells	1.19–1.33	2.94–3.33	0.60–1.21
7	$\text{nBu}_3\text{SnCl}(\text{C}_2\text{H}_5\text{OH})_2$ –whole erythrocytes, –membranes, and –ghost cells	1.21–1.37	2.96–3.39	0.80–1.57
8	$\text{Ph}_2\text{SnCl}_2(\text{C}_2\text{H}_5\text{OH})_2$ –whole erythrocytes, –membranes, and –ghost cells	0.95–1.13	2.47–2.96	0.98–1.16
9	$\text{Ph}_3\text{SnCl}(\text{C}_2\text{H}_5\text{OH})_2$ –whole erythrocytes, and –ghost cells	1.12–1.19	2.75–2.83	1.13–1.50

<sup>a</sup> At liquid-nitrogen temperature. Data from Ref. 27<sup>b</sup> Samples prepared as described in the Experimental section: methyltins from aqueous solutions at physiological pH,  $\text{Me}_2\text{Sn}(\text{OH})_2$  and  $\text{Me}_3\text{Sn}(\text{OH})(\text{OH}_2)$ , and organotins from ethanol,  $\text{R}_n\text{SnCl}_{4-n}(\text{C}_2\text{H}_5\text{OH})_m$ , reacted with erythrocytes, from which pellets of organotin–cell membrane were subsequently obtained by hemolysis. Ghost cells were prepared by previous hemolysis of erythrocytes, and then reacted with the above solutions of organotins.<sup>c</sup> See footnotes c and d to Table 1.<sup>d</sup> Full width at half-height of the resonant peaks; ranges of 'working' values from computer fitting.

crystallographic studies and the corresponding estimates from the point-charge model treatment of Mössbauer  $\Delta E$  parameters, for the following classes of model compounds: (i)  $\text{R}_2\text{Sn}$ –dipeptide

**Figure 2** The structures assigned<sup>27</sup> to the organotin–erythrocytes and related systems through fingerprint criteria (Table 1) concerning experimental values of nuclear quadrupole splitting  $\Delta E$  (Table 3), and point-charge model calculations of angles according to the procedure (II). A', A'' and A''' are electronegative bonding atoms, e.g. O, N.

(Fig. 3); (ii)  $\text{R}_3\text{Sn}$ –acetyldipeptide (Fig. 4); (iii)  $\text{R}_2\text{Sn}$ –carbohydrates and  $\text{R}_2\text{Sn}$ –nucleosides (Fig. 5); (iv)  $\text{Me}_2\text{Sn}(\text{OH})_2$  and  $\text{Me}_3\text{Sn}(\text{OH})(\text{OH}_2)$  in aqueous solutions in the presence of excess dimethylphosphinate or cyclic adenosine-3':5'-phosphate (Fig. 6); (v)  $\text{R}_2\text{Sn}$ – and  $\text{R}_3\text{Sn}$ –phosphate complexes (Fig. 7). These data, when compared with the  $\Delta E$  parameters and the representative angles reported in Table 3 and Fig. 2, suggest that the organotin–erythrocytes and organotin–erythrocyte membrane systems 1, 2, and 4–7 could consist of five-coordinated

**Figure 3** The structure (idealized) of  $\text{R}_2\text{Sn}$ –dipeptide complexes. C–Sn–C angles from X-ray diffractometry<sup>48–53</sup> are as follows: for R = Alk, C–Sn–C = 121.7–131.4°; for R = Ph, C–Sn–C = 117.5°. C–Sn–C angles from  $\Delta E_{\text{exp}}$  data<sup>35, 52–55</sup> and point-charge model (II) estimates are: for R = Alk, solid-state and frozen solutions,  $\Delta E_{\text{exp}} = 2.46–3.51$  mm s<sup>-1</sup>, C–Sn–C = 104–133°; for R = Ph, solid-state,  $\Delta E_{\text{exp}} = 2.21–2.39$  mm s<sup>-1</sup>, C–Sn–C = 108–114°.

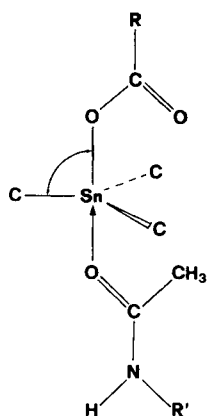


**Figure 4** A possible tin environment in complexes  $R_3Sn$ -*N*-acetyldipeptide in the solid state; R = Me, Et, nBu, nOct, Cy, Ph; dipeptide = glycylglycine, glycylalanine, glycylvaline.<sup>56</sup>

C-Sn-O angles from  $\Delta E_{\text{exp}}$  data<sup>56</sup> and point-charge model (II) estimates: for R = Alk,  $\Delta E_{\text{exp}} = 3.29$ – $3.66 \text{ mm s}^{-1}$ , C-Sn-O =  $95$ – $90^\circ$ ; for R = Ph,  $\Delta E_{\text{exp}} = 3.12$ – $3.17 \text{ mm s}^{-1}$ , C-Sn-O  $\approx 90^\circ$ .

$\text{Alk}_3\text{Sn}^{\text{IV}}$  and  $\text{Alk}_3\text{Sn}^{\text{IV}}$  moieties bound to electro-negative donor atoms, such as oxygen and nitrogen, from protein side chain fragments or from protein constituents (Figs 3 and 4). Moreover, systems 1, 2 and 6 could consist of  $\text{Alk}_2\text{Sn}^{\text{IV}}$  moieties bound to hydroxyl oxygen atoms of carbohydrates (Fig. 5), although the molecular structure of these solid-state complexes<sup>57–59</sup> may hardly be assumed to be duplicated in our organotin-erythrocyte systems. Lastly, organotins in systems 1 and 4 could form adducts with phosphodiester fragments (Fig. 6); on the other hand, 2, 3 and 5–9 cannot consist of phosphate complexes such as those in Fig. 7.

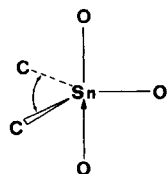


**Figure 5** The nature of the environment of tin atoms in derivatives of carbohydrates (five-coordinated tin sites) and of nucleosides. C-Sn-C angles in  $\text{nBu}_2\text{Sn}$ -1,3,2-dioxastannolanes, glucose and mannose derivatives, are in the range  $125.8$ – $139^\circ$ , as determined by X-ray diffractometry<sup>57–59</sup> (C-Sn-C =  $137.9^\circ$  in  $\text{nBu}_2\text{Sn}$ -1,3,2-dioxastannolane, mannose, six-coordinate tin site<sup>58,59</sup>). C-Sn-C angles from  $\Delta E_{\text{exp}}$  data<sup>59–61</sup> and point-charge model (II) estimates for  $\text{nBu}_2\text{Sn}$ -1,3,2-dioxastannolane, glucose and mannose derivatives:  $\Delta E_{\text{exp}} = 2.38$ – $2.78 \text{ mm s}^{-1}$ , C-Sn-C  $\approx 100$ – $114^\circ$ ; for  $\text{Alk}_2\text{Sn}$ -nucleosides,  $\Delta E_{\text{exp}} = 2.97$ – $3.24 \text{ mm s}^{-1}$ , C-Sn-C =  $119$ – $127^\circ$ .

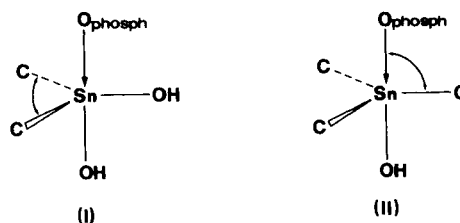


**Figure 6** Possible tin environments in  $\text{Me}_2\text{Sn}(\text{OH})_2$  and  $\text{Me}_3\text{Sn}(\text{OH})(\text{OH}_2)$  in the presence of excess dimethylphosphinate or cyclic adenosine-3':5'-phosphate (both characterized by  $\text{R}_2\text{PO}_2^-$  groups), in aqueous solution at physiological pH.<sup>33</sup>  $\text{O}_{\text{phosph}}$  stands for coordinated phosphate oxygen. C-Sn-C and C-Sn-O angles from  $\Delta E_{\text{exp}}$  data<sup>33</sup> and point-charge model (II) estimates: for I,  $[\text{ligand}]/[\text{Me}_2\text{Sn}(\text{OH})_2] = 9.97, 8.14$ ;  $\Delta E_{\text{exp}} = 2.70, 2.72 \text{ mm s}^{-1}$ ; C-Sn-C =  $113^\circ$ ,<sup>33</sup> for II,  $[\text{ligand}]/[\text{Me}_3\text{Sn}(\text{OH})(\text{OH}_2)] = 8.46, 9.85$ ;  $\Delta E_{\text{exp}} = 3.02, 3.26 \text{ mm s}^{-1}$ ; C-Sn-O =  $107^\circ, 105^\circ$ .<sup>33</sup>

It seems worthwhile to comment here on the  $^{119}\text{Sn}$  Mössbauer response from organotin-cell membrane systems and related models reported in the literature. In membranes of rat liver mitochondria,  $\text{Et}_3\text{Sn}^{\text{IV}}$  has been assumed to bind to thiol sulfur, and/or to heterocyclic nitrogen from histidine, forming tetrahedral species, or trigonal-bipyramidal species with facial  $\text{SnC}_3$  fragments ( $\delta = 1.49, 1.22 \text{ mm s}^{-1}$ ;  $\Delta E = 2.78, 1.67 \text{ mm s}^{-1}$ , respectively<sup>11,12</sup>); moreover, a trigonal-bipyramidal species  $\text{Et}_3\text{SnA}_2$  ( $\delta = 1.56 \text{ mm s}^{-1}$ ,  $\Delta E = 3.44 \text{ mm s}^{-1}$ ) would constitute the fraction dissolved into the mitochondrial membrane.<sup>11,12</sup> The latter  $\Delta E$  parameter corresponds to  $\Delta E$  data of our systems 4, 5 and 7 (Table 3 and Fig. 2), involving  $\text{Alk}_3\text{Sn}^{\text{IV}}$  moieties, where no evidence was obtained for the occurrence of tetrahedral

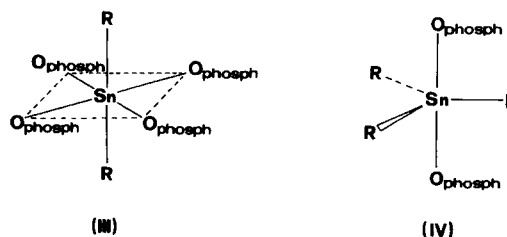


**Figure 7** The structures of  $\text{R}_2\text{Sn}[\text{PO}_2(\text{XY})]_2$ <sup>62–69</sup> and  $\text{R}_3\text{Sn}[\text{PO}_2(\text{XY})]$  complexes<sup>63, 66–68, 70–72</sup>.

III: X = Y = H, Cl, OPh, OEt,  $\text{C}_6\text{H}_{13}$ ; X = H, Y = Ph; X = OPh, Y = Ph. For R = Alk,  $\Delta E_{\text{exp, av}} = 4.60 \text{ mm s}^{-1}$ ,<sup>63–69</sup> for R = Ph,  $\Delta E_{\text{exp, av}} = 4.08 \text{ mm s}^{-1}$ .<sup>62, 67, 68</sup>

IV: X = Y = H, Cl, Ph, OPh, OSn-nBu<sub>3</sub>, Me,  $\text{C}_6\text{H}_{13}$ ; X = Me, Y = OSn-nBu<sub>3</sub>; X = Ph, Y = OSn-nBu<sub>3</sub>, OPh, H. For R = Alk,  $\Delta E_{\text{exp, av}} = 3.90 \text{ mm s}^{-1}$ ,<sup>63, 66–68, 70–72</sup> for R = Ph,  $\Delta E_{\text{exp, av}} = 3.49 \text{ mm s}^{-1}$ .<sup>67, 68, 71</sup>

**Table 4**  $^{119}\text{Sn}$  Mössbauer parameters of organotin(IV)–rat hemoglobin systems<sup>a</sup>

System no.	Organotin compounds reacted with hemoglobin <sup>b</sup>	$r^c$	$\delta$ (mm s <sup>-1</sup> ) <sup>d</sup>	$\Delta E$ (mm s <sup>-1</sup> ) <sup>d</sup>	$\Gamma_1, \Gamma_2$ (mm s <sup>-1</sup> ) <sup>d</sup>
10	$\text{Me}_2\text{Sn}(\text{OH})_2 \cdot \text{Hepes}$	1.81; 1.18	1.19; 1.24	2.23; 2.30	0.84–1.32
11	$\text{Me}_2\text{Sn}(\text{OH})(\text{GlyGly}) \cdot \text{Hepes}^e$	1.76; 1.40	1.29; 1.28	2.23; 2.10	0.97–1.53
12	$\text{Me}_2\text{Sn}(\text{OH})[\text{SCH}_2\text{CH}(\text{NH}_3^+)\text{COO}^-]$	1.83; 1.44	1.16; 1.33	2.19; 2.39	0.93; 1.12
13	$[\text{Me}_2\text{Sn}(\text{SCH}_2\text{CH}_2\text{SO}_3)_2]^{2- f}$	1.05–2.07	1.33–1.35	1.58–1.71	0.57–1.06
14	$\text{Me}_2\text{Sn}[\text{SCH}_2\text{CH}(\text{NH}_3^+)\text{COO}^-]_2$	1.45	1.27	2.21	0.83; 0.96
15	$\text{Me}_2\text{Sn}[\text{SC}(\text{CH}_3)_2\text{CH}(\text{NH}_3^+)\text{COO}^-]_2$	0.97	1.23	2.48	0.70; 0.83
16	$\text{Me}_3\text{Sn}(\text{OH}) \cdot \text{Hepes}$	1.90; 2.00	1.25; 1.32	1.53; 1.57	0.70–1.03
17	$\text{Et}_3\text{Sn}(\text{OH}) \cdot \text{Hepes}^g$	1.83–1.95	1.38–1.48	1.61–1.78	0.74–0.88
18	$\text{nBu}_3\text{Sn}(\text{OH})$	0.73–2.35	1.45–1.50	1.77–1.94	0.63–1.03

<sup>a</sup> At liquid-nitrogen temperature. Data from Refs 15, 17–19.<sup>b</sup> Samples prepared as described in the Experimental section; see Table 2(B) for the parameters of the reactant species in Hepes buffer. Nos 10–12, 14, 15 refer to samples obtained by co-crystallization of the organotin compounds and hemoglobin, while Nos 13, 16–18 concern samples from both co-crystallization and diffusion of aqueous organotins into crystalline hemoglobin (see the Experimental section).<sup>c</sup>  $r = [\text{Sn}]/[\text{hemoglobin tetramer}]$ ; estimated by visible spectrophotometry analysis of pellets for  $\text{R}_n\text{Sn}^{\text{IV}}$  and hemoglobin contents for  $\text{Et}_3\text{Sn}^{\text{IV}}$ – and  $\text{Bu}_3\text{Sn}^{\text{IV}}$ –hemoglobin.<sup>17</sup><sup>d</sup> See footnotes c, d to Table 1, and d to Table 2.<sup>e</sup> Glygly = glycylglycinate.<sup>f</sup> Sodium and guanidinium salts.<sup>g</sup> Includes the data for a sample  $(\text{Et}_3\text{Sn})_2(\text{feline hemoglobin})$ .<sup>15</sup>

species, and consequently for binding to thiol groups, which instead generally occurs in rat hemoglobin derivatives (*vide infra*). Moreover,  $\text{Ph}_3\text{Sn}^{\text{IV}}$  in cell walls of *Ceratocystis ulmi* yields<sup>73</sup>  $\delta = 1.23 \text{ mm s}^{-1}$ ,  $\Delta E = 3.06\text{--}3.13 \text{ mm s}^{-1}$ , which suggests the occurrence of trigonal-bipyramidal species  $\text{Ph}_3\text{SnA}_2$  (Table 1) analogously to our  $\text{Ph}_3\text{Sn}^{\text{IV}}$  system 9 (Table 3 and Fig. 2).

In the study by Farrow and Dawson<sup>11</sup> referred to above, the binding sites for  $\text{Et}_3\text{Sn}^{\text{IV}}$  in rat liver mitochondria were investigated at different triethyltin incubation concentrations in the range  $8.9\text{--}35.7 \text{ nmol (mg of protein)}^{-1}$ ; the increase of the amount of  $\text{Et}_3\text{Sn}^{\text{IV}}$  induces a parallel increase of the species  $\text{Et}_3\text{SnA}_2$ .<sup>11</sup> In *Ceratocystis ulmi*, for example,  $12.9 \text{ mmol of Ph}_3\text{SnCl}$  is added to  $5 \times 10^{-6}$  cells ( $5 \text{ cm}^3$  of packed cells).<sup>73</sup> In our present study we have employed systems consisting of  $0.7\text{--}7.6 \text{ }\mu\text{mol of organotin per mg protein}$  or, for example,  $30 \text{ }\mu\text{mol of organotin per } 3 \text{ cm}^3$  of packed erythrocytes or ghosts, in the incubations; these ratios are intermediate between those referred to above for mitochondria and fungi, and correspond to the conditions employed in the study of the interaction of  $\text{Me}_3\text{Pb}^{\text{IV}}$  with glutathione in human erythrocytes ( $1 \text{ }\mu\text{mol of organolead per } 0.4 \text{ cm}^3$  of packed cells<sup>74</sup>).

It is concluded that our systems, generally involving trigonal-bipyramidal organotin complexes with erythrocyte membranes and cytoplasm, correspond to Farrow's species dissolved in the mitochondrial membrane; these systems may be consistent with the simultaneous presence of a series of species, originated by bonding to tin of the biological donors in Figs 3–6, as well as by micelles intercalated into lipid bilayers and formed for example by trigonal-bipyramidal hydrolysis products of organotins, or by other types of coordination. The assumption of multiple tin sites is supported by the magnitude of the linewidths,  $\Gamma$ , of the Mössbauer resonant signals, which often exceed  $1 \text{ mm s}^{-1}$ , in a special way for the  $\text{Me}_2\text{Sn}^{\text{IV}}$  systems 2 and 3 (which is consistent for example with the formation of both trigonal-bipyramidal and octahedral species reported in Fig. 2), as well as for the  $\text{nBu}_3\text{Sn}^{\text{IV}}$  and  $\text{Ph}_3\text{Sn}^{\text{IV}}$  species 7 and 9 (Table 3). It therefore seems to us that the important conclusion reached in the present investigation consists in the general occurrence of five-coordination in our erythrocyte systems. Further work is clearly needed in order possibly to identify individual binding sites, concerning specific ligand atoms from the biological constituents. The possible bonding by thiol sulfur

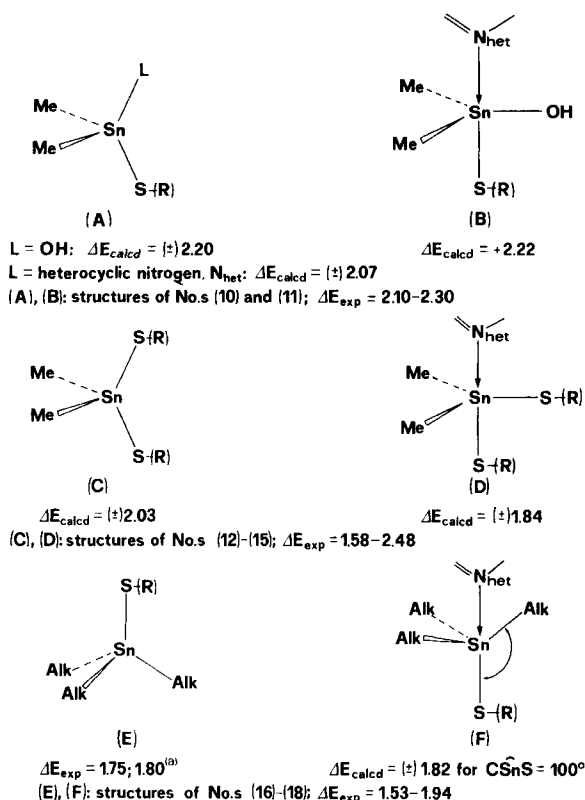


**Figure 8** The structures assigned<sup>17–19</sup> to the organotin–rat hemoglobin systems 10–18 through correlation of the experimental  $\Delta E$  values (Table 4) with point-charge model calculations,  $\Delta E_{calcd}$ ,  $\text{mm s}^{-1}$ ,<sup>17–19</sup> effected according to the literal version [(I); Experimental section, this paper]. Heterocyclic nitrogen atoms, from histidine side chains for example, are indicated  $N_{het}$ , and thiol groups  $S(R)$ . Structures A–E are regular; (F) is distorted at the C–Sn–C angles.

<sup>a</sup> Ref. 17.

would be investigated at the level of nanomolar organotin per mg of membrane protein, according to studies on mitochondrial membranes.<sup>11</sup>

### Organotin–rat hemoglobin

The Mössbauer parameters<sup>17–19</sup> are summarized in Table 4. Isomer shifts ( $\delta$ ) are typically in the ranges usually shown by dialkyltin and trialkyltin derivatives.<sup>28–32, 34</sup> The linewidths ( $\Gamma$ ) are generally less than  $1 \text{ mm s}^{-1}$ , consistent with the occurrence of single tin sites. Fingerprint criteria for  $\Delta E$  data (Table 1) indicate tetrahedral tin environments for all the hemoglobin derivatives 10–18. It follows that the trigonal-bipyramidal organotin  $\text{Me}_2\text{Sn}(\text{OH})_2$ . Hepes,  $\text{Alk}_3\text{Sn}(\text{OH})(L)$ ,  $n\text{Bu}_3\text{SnOH}$ , and related species [Table 2(B)] react fully with the protein.

Due to the non-zero value of the partial nuclear quadrupole splitting of thiol sulfur,<sup>18</sup> point-charge model calculations on the structures related to organotin–feline hemoglobin and rat hemoglobin complexes (characterized by the occurrence of Sn–S bonds; see Introduction) have been made by the literal version (I), where all bonds to tin are accounted for (see the Experimental section of this paper). The point-charge model structures thus obtained, yielding  $\Delta E_{calcd}$  values in agreement with the  $\Delta E_{exp}$  data (Table 4), are reported in Fig. 8. The related data for model systems in solution phases and in the solid state are referred to in Figs 9 and 10.

The reaction of rat hemoglobin with  $\text{Me}_2\text{Sn}^{\text{IV}}$ , as well as of its complexes with electronegative donors such as the peptide nitrogen atoms of glycylglycine,<sup>18, 35</sup> in aqueous systems at physiological pH (systems 10 and 11, Table 4), could yield complexes with tin environments as in A or B, Fig. 8.<sup>18</sup>

The possible tetrahedral environments (A) are in line with assumptions on  $\text{R}_3\text{Sn}^{\text{IV}}$ –hemoglobin in solution.<sup>15, 86</sup> Bonding by both thiol sulfur and heterocyclic nitrogen (B) corresponds to the structural assumptions for  $(\text{Et}_3\text{Sn})_2$ (hemoglobin tetramer), the axial location of thiol sulfur being dictated by conformational constraints.<sup>20</sup> In fact, model aqueous systems with  $\text{Me}_2\text{Sn}[\text{SCH}_2\text{CH}(\text{NH}_2)\text{COO}]$ ,  $\text{Me}_2\text{Sn}[\text{SC}(\text{CH}_3)_2\text{CH}(\text{NH}_2)\text{COO}]$  and  $\text{Me}_2\text{Sn}(\text{SCH}_2\text{CH}_2\text{SO}_3)$  clearly assume structure G, (Fig. 9) with equatorial thiol sulfur and axial hydroxyl and amino nitrogen (the latter being the more electronegative bonding atoms), according to the Muetterties rule on five-coordinated configurations.<sup>87</sup>

Mono- and bis-thiolate derivatives of  $\text{Me}_2\text{Sn}^{\text{IV}}$  (12–15, Table 4) react with rat hemoglobin, apparently occurring as bithiolates in the hemoglobin ‘phase’, with the tetrahedral or trigonal-bipyramidal configurations C or D (Fig. 8).<sup>18, 19</sup> Bithiolates in the hemoglobin systems 13–15 have been assumed as tetrahedral species C, linked to the protein by Coulomb and hydrogen bonds formed by the sulfonate and amino-acid residues,<sup>19</sup> analogous to literature reports.<sup>88–90</sup> In fact the model aqueous systems  $\text{Me}_2\text{Sn}[\text{SCH}_2\text{CH}(\text{NH}_3^+)\text{COO}^-]_2$ ,  $\text{Me}_2\text{Sn}[\text{SC}(\text{CH}_3)_2\text{CH}(\text{NH}_3^+)\text{COO}^-]_2$  and  $[\text{Me}_2\text{Sn}(\text{SCH}_2\text{CH}_2\text{SO}_3)_2]^{2-}$  would either assume the trigonal-bipyramidal structure H (Fig. 9) or the tetrahedral structure J (Fig. 10) in Hepes buffer, whilst  $[\text{R}_2\text{Sn}(\text{SCH}_2\text{CH}_2\text{SO}_3)_2]^{2-}$  appear to adopt the tetrahedral form J (Fig. 10) in the solid state (R = Me, Ph) and in aqueous



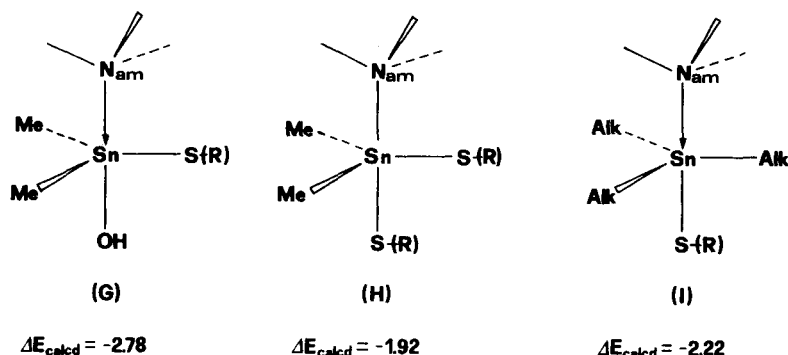


**Figure 9** The (regular) trigonal-bipyramidal structures assigned to model systems  $\text{Me}_2\text{Sn}^{\text{IV}}$ -monothiolates and  $\text{Me}_2\text{Sn}^{\text{IV}}$ -dithiolates, and  $\text{Alk}_3\text{Sn}^{\text{IV}}$ -thiolates ( $\text{Alk} = \text{Me}, \text{Et}$ ) in aqueous solution at physiological pH, optionally in the presence of Hepes buffer (coordinating through amino nitrogen atoms,  $\text{N}_{\text{am}}$ ).  $\Delta E_{\text{calcd}}$  values ( $\text{mm s}^{-1}$ ) have been estimated by the literal version of the point-charge model, (I). Model systems, and related  $\Delta E_{\text{exp}}$  parameters, are as follows:

- G:**  $\text{Me}_2\text{Sn}^{\text{IV}}$ -cysteine,  $\text{Me}_2\text{Sn}^{\text{IV}}$ -2-mercaptoethanesulfonate,  $\text{Me}_2\text{Sn}^{\text{IV}}$ -penicillamine, 1:1, in Hepes;  $\Delta E_{\text{exp}} = 2.63\text{--}2.91 \text{ mm s}^{-1}$ .<sup>18, 75, 76</sup>
- G:**  $\text{Me}_2\text{Sn}^{\text{IV}}$ -cysteine, 1:1, in  $\text{H}_2\text{O}$ ,  $\text{pH} = 7.5\text{--}9.5$ ;  $\Delta E_{\text{exp, av}} = 2.57 \text{ mm s}^{-1}$ .<sup>77</sup> The axial amino nitrogen atom is from the amino group of cysteine.<sup>77</sup>
- H:**  $\text{Me}_2\text{Sn}^{\text{IV}}$ -cysteine,  $\text{Me}_2\text{Sn}^{\text{IV}}$ -2-mercaptoethanesulfonate,  $\text{Me}_2\text{Sn}^{\text{IV}}$ -penicillamine, 1:2–1:4, in Hepes;  $\Delta E_{\text{exp}} = 1.97\text{--}2.63 \text{ mm s}^{-1}$ .<sup>18, 75, 78</sup> Tetrahedral structures (J) (Fig. 10) have been also advanced.<sup>75, 78</sup>
- I:**  $\text{Me}_3\text{Sn}^{\text{IV}}$ -cysteine and  $\text{Et}_3\text{Sn}^{\text{IV}}$ -cysteine, 1:1, in Hepes;  $\Delta E_{\text{exp}} = 2.44, 2.59 \text{ mm s}^{-1}$ .<sup>17</sup> These values are essentially unchanged for molar ratios 1:2–1:3.<sup>17</sup>

solution.<sup>18, 75, 78</sup> It is worthy of note that the saturated complexes are characterized by the  $\text{C}_2\text{SnS}_2$  skeleton<sup>18, 75, 78</sup> (H) (Fig. 9), there being no evidence for further tin coordination by thiol sulfur.

Triorganotin species are likely to yield the environment E (Fig. 8) in hemoglobin complexes, as viewed from the magnitude of the parameters  $\Delta E$  of 16–18 (Table 4); this assumption is in line with literature reports.<sup>15, 86</sup> The latter structure is typically assumed by a series of thiolates  $\text{R}_3\text{SnSR}$  in the solid state and in solution phases<sup>17, 75, 79–83</sup> (K, Fig. 10). The assumption of trigonal-bipyramidal configurations implies a severe distortion from the ideal geometry in order to account for the  $\Delta E_{\text{exp}}$  data (F, Fig. 8);<sup>17</sup> in fact, the experimental and calculated parameters  $\Delta E$  for regular trigonal-bipyramidal model systems in solution and in the solid state (I and L, Figs 9 and 10) are inconsistent with  $\Delta E$  data for the hemoglobin complexes. It is noteworthy that I and L are saturated complexes, occurring in excess of both thiol sulfur and nitrogen ligands.<sup>17, 84, 85</sup>

Axial coordination by two heterocyclic nitrogen atoms in  $\text{R}_3\text{Sn}$ -hemoglobin is excluded by point-charge model calculations, the related parameter being<sup>91</sup>  $\Delta E_{\text{calcd}} = -3.25 \text{ mm s}^{-1}$ ; the possible occurrence of facial as well as meridional fragments  $\text{SnC}_3$ <sup>91</sup> is ruled out by the value of the

asymmetry parameter  $\eta = 0.00$  determined from the Mössbauer–Zeeman spectra of the  $(\text{Et}_3\text{Sn})_2(\text{hemoglobin tetramer})$ .<sup>17</sup>

## CONCLUSIONS

The water soluble organotin(IV) species  $\text{Me}_2\text{Sn}(\text{OH})_2$ ,  $\text{Me}_3\text{Sn}(\text{OH})(\text{OH}_2)$  and  $\text{Et}_3\text{Sn}(\text{OH})(\text{OH}_2)$ , formed at physiological pH, react with thiol groups of biological molecules, yielding products characterized by covalent Sn–S bonds, with stoichiometries corresponding to  $[\text{R}_2\text{Sn}(\text{SR}')^+]^+$ ,  $\text{R}_2\text{Sn}(\text{SR}')_2$  and  $\text{R}_3\text{SnSR}'$ . Ligand molecules with electronegative donor atoms, such as amino nitrogen and phosphate oxygen, appear to produce labile adducts with, for example,  $\text{Me}_2\text{Sn}(\text{OH})_2$  and  $\text{Me}_3\text{Sn}(\text{OH})(\text{OH}_2)$ , in aqueous solution at  $\text{pH} \approx 7$ , for large ligand-to-metal molar ratios.

These assumptions are in line with potentiometric studies on hydrolysis and stability constants of methyltin(IV) moieties.<sup>92, 93</sup> Consequently, one is tempted to assume that water-soluble organotin moieties preferentially occur in biological systems in the form of the thiol species

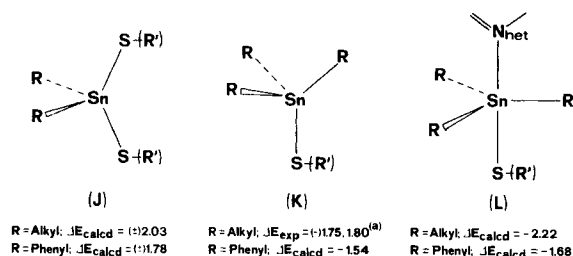


**Figure 10** The (regular) tetrahedral and trigonal-bipyramidal structures attributed to model systems  $R_2\text{Sn}^{\text{IV}}$ -dithiolates and  $R_3\text{Sn}^{\text{IV}}$ -thiolates,  $R = \text{Alk, Ph}$ , in the solid state as well as in solution phase (aqueous or organic). The literal version of the point-charge model, (I), has been employed for the estimate of  $\Delta E_{\text{calcd}}$  in  $\text{mm s}^{-1}$ . The model systems, and the respective parameters, are as follows.

- J:**  $R_2\text{Sn}[\text{S}(\text{CH}_2)_2\text{SO}_3^-]_2$ , sodium and guanidinium salts. Solid-state:  $R = \text{Me}$ ,  $\Delta E_{\text{exp}} = 1.66, 1.68 \text{ mm s}^{-1,75}$ ;  $R = \text{Ph}$ ,  $\Delta E_{\text{exp}} = 1.44, 1.67 \text{ mm s}^{-1,75}$ . Aqueous solution,  $\text{pH} = 6.6\text{--}7.4$ ;  $R = \text{Me}$ ,  $\Delta E_{\text{exp}} = 1.84 \text{ mm s}^{-1,75}$ .
- K:**  $R_3\text{Sn}(\text{SR}')$ . Solid-state:  $R = \text{Alk}$ ,  $\Delta E_{\text{exp}} = 1.40\text{--}1.76 \text{ mm s}^{-1,75,79\text{--}82}$ ;  $R = \text{Ph}$ ,  $\Delta E_{\text{exp}} = 1.20\text{--}1.42 \text{ mm s}^{-1,17,80,82,83}$  [ $\text{SR}' = \text{SCH}_2\text{COO}^-$ ,  $\text{S}(\text{CH}_2)_3\text{CH}(\text{NHR}'')\text{COO}^-$ , glutathione,  $\text{S}(\text{CH}_2)_2\text{SO}_3^-$ ]. Aqueous solution,  $\text{pH} = 7.4$ :  $R = \text{Me}$ ,  $\Delta E_{\text{exp}} = 1.42 \text{ mm s}^{-1,75}$  [ $\text{SR}' = \text{S}(\text{CH}_2)_2\text{SO}_3^-$ ]. Benzene solution,  $R = \text{Alk}$ ,  $\Delta E = 1.97, 2.06 \text{ mm s}^{-1}$ ;  $R = \text{Ph}$ ,  $\Delta E = 1.37, 1.46 \text{ mm s}^{-1,17}$  [ $\text{SR}' = \text{SC}_6\text{H}_5$ , 8-thioquinoline].
- L:**  $R_3\text{Sn}(\text{SR}')$  + ligand in benzene, and  $R_3\text{Sn}(\text{SR}')$  in pyridine.  $R = \text{Alk}$ ,  $\Delta E = 2.62\text{--}2.78 \text{ mm s}^{-1,17,84}$ ;  $R = \text{Ph}$ ,  $\Delta E = 2.34\text{--}2.54 \text{ mm s}^{-1,17,84,85}$  ( $\text{SR}' = \text{SC}_6\text{H}_5$ , 4-thiopyridine; ligand = *N*-methylimidazole).

<sup>a</sup> Ref. 17.

referred to above. The biological activity of organotin compounds would then be ascribed to the molecules above, or to the original hydrolysis products, in the present context. In fact, effects due to organotin thiolates have been reported earlier.<sup>76,77,94,95</sup> It seems somewhat unrealistic to transfer totally into biological environments results concerning chemical bonding and reactivity in aqueous solutions. Moreover, the possible correlation with real biological processes of our *in vitro* interactions by ethanolic organotin chlorides with erythrocytes and native DNA has still to be investigated, and the biological effects possibly induced by water-insoluble (e.g. micellar) hydrolyzed organotin compounds have still to be determined.

**Acknowledgements** Financial support by Consiglio Nazionale delle Ricerche, Roma, Progetto Finalizzato Chimica Fine II, and by MURST, Progetti di Interesse nazionale (40%), is acknowledged.

## REFERENCES

1. Porvaznik, M, Gray, B H, Mattie, D, Jackson, A G and Omlor, R R *Lab. Invest.*, 1986, 54: 254
2. Gray, B H, Porvaznik, M and Lee, L H *J. Appl. Toxicol.*, 1986, 6: 263; Gray, B H, Porvaznik, M, Lee, L H and Flemming, C J *J. Appl. Toxicol.*, 1986, 6: 363
3. Otera, J, Ioka, S and Nozaki, H *J. Org. Chem.*, 1989, 54: 4013
4. Selwyn, M J, Dawson, A P, Stockdale, M and Gains, N *Eur. J. Biochem.*, 1970, 14: 120
5. Motais, R, Cousin, J L and Sola, F *Biochim. Biophys. Acta*, 1977, 467: 357
6. Vieth, J O and Tosteson, M T *J. Gen. Physiol.*, 1979, 73: 765
7. Tosteson, M T and Vieth, J O *J. Gen. Physiol.*, 1979, 73: 789
8. Siebenlist, K R and Taketa, F *Toxicol. Appl. Pharmacol.*, 1981, 58: 67
9. Ali, A A, Upreti, R K and Kidway, A M, *Toxicol. Lett.*, 1987, 38: 13; Ali, A A, Upreti, R K and Kidway, A M *Bull. Environ. Contam. Toxicol.*, 1990, 44: 29
10. Zucker, R M, Elstein, K H, Easterling, R E, Ting-Beall, H P, Allis, J W and Massaro, E J *Toxicol. Appl. Pharmacol.*, 1988, 96: 393
11. Farrow, B G and Dawson, A P, *Eur. J. Biochem.*, 1978, 86: 85
12. Dawson, A P, Farrow, B G and Selwyn, M J, *Biochem. J.*, 1982, 202: 163
13. Aldridge, W N and Street, B W, *Biochem. J.*, 1964, 91: 287
14. Heywood, B R, Molloy, K C and Waterfield, P C *Appl. Organomet. Chem.*, 1989, 3: 443
15. Elliot, B M, Aldridge, W N and Bridges, J W *Biochem. J.*, 1979, 177: 461
16. Siebenlist, K R and Taketa, F *Biochem. J.*, 1986, 233: 471
17. Barbieri, R, Silvestri, A, Lo Giudice, M T, Ruisi, G and Musmeci, M T *J. Chem. Soc., Dalton Trans.*, 1989: 519
18. Barbieri, R and Musmeci, M T, *J. Inorg. Biochem.*, 1988, 32: 89
19. Barbieri, R and Musmeci, M T *Phosphorus, Sulfur, and Silicon*, 1990, 53: 103
20. Chu, A L, Taketa, F, Mauk, A G and Brayer, G D *J. Biomol. Struct. Dyn.*, 1985, 3: 579
21. Rose, M S, *Biochem. J.*, 1969, 111: 129
22. Li, A P, Dahl, A R and Hill, J O, *Toxicol. Appl. Pharmacol.*, 1982, 64: 482
23. Westendorf, J, Marquardt, H and Marquardt, H *Arzneim.-Forsch., Drug Res.*, 1986, 36(II): 1263
24. Sagelsdorff, P, Dollenmeyer, P, Ebner, D, Bieri, F, Kelly, S M, Stäubli, W, Waechter, F and Bentley, P *Toxicol. Lett.*, 1990, 50: 179
25. Barbieri, R and Silvestri, A *J. Inorg. Biochem.*, 1991, 41: 31
26. Barbieri, R, Silvestri, A, Giuliani, A M, Piro, V, Di Simone, F and Madonia, G *J. Chem. Soc., Dalton Trans.*, in the press; Barbieri, R and Silvestri, A *Inorg., Chim. Acta*, 1991, 188: 95; Piro, V, Di Simone, F, Madonia, G,

- Silvestri, A, Giuliani, A M, Ruisi, G and Barbieri, R *Appl. Organomet. Chem.*, 1992, 6: 000
27. Musmeci, M T, Madonia, G and Barbieri, R Unpublished results
28. Clark, M G, Maddock, A G and Platt, R H J. *Chem. Soc., Dalton Trans*, 1972: 281
29. Sham, T K and Bancroft, G M *Inorg. Chem.*, 1975, 14: 2281
30. Parish, R V In: *Mössbauer Spectroscopy Applied to Inorganic Chemistry*, Long, G J (ed), Plenum, New York, 1984, vol 1, pp 527-575
31. Bancroft, G M and Platt, R H, *Adv. Inorg. Chem. Radiochem.*, 1972, 15: 59
32. Bancroft, G M, Kumar Das, V G, Sham, T K and Clark, M G *J. Chem. Soc., Dalton Trans*, 1976: 643
33. Barbieri, R, Silvestri, A and Piro, V *J. Chem. Soc., Dalton Trans*, 1990: 3605
34. Smith, P J, *Organomet. Chem. Rev. A*, 1970, 5: 373
35. Ruisi, G, Silvestri, A, Lo Giudice, M T, Barbieri, R, Atassi, G, Huber, F, Grätz, K and Lamartina, L, *J. Inorg. Biochem.*, 1985, 25: 229
36. Harrison, P G, Begley, M J and Molloy, K C *J. Organomet. Chem.*, 1980, 186: 213
37. Brown, J M, Chapman, A C, Harper, R, Mowthorpe, D J, Davies, A G and Smith, P J *J. Chem. Soc., Dalton Trans*, 1972: 338
38. Edelmann, M A, Hitchok, P B and Lappert, M F, *J. Chem. Soc., Chem. Comm.*, 1990: 1116
39. Glydewell, C and Liles, D C, *Acta Cryst.*, 1978, B34: 1693; Glydewell, C and Liles, D C *Acta Cryst.*, 1979, B35: 1689; Glydewell, C and Liles, D C *J. Chem. Soc., Chem. Comm.*, 1979: 93
40. Kersch, S, Wrackmeyer, B, Männing, D, Nöth, H and Staudigl, R *Z. Naturforsch.*, 1987, 42B: 387
41. Lockhart, T P, Puff, H, Schuh, W, Reuter, H and Mitchell, T N *J. Organomet. Chem.*, 1989, 366: 61
42. Chow, J M, *Inorg. Chem.*, 1971, 10: 673
43. Graziani, G, Casellato, U and Plazzogna, G *Acta Cryst.*, 1983, C39: 1188
44. Vollano, J F, Day, R O and Holmes, R R *Organometallics*, 1984, 3: 745
45. Alcock, N W, Pennington, M and Willey, G R, *J. Chem. Soc., Dalton Trans*, 1985: 2683
46. Kasai, N, Yasuda, M and Okawara, R *J. Organomet. Chem.*, 1965, 3: 172
47. Glydewell, C and Liles, D C, *Acta Cryst.*, 1978, B34: 129
48. Huber, F, Haupt, H J, Preut, H, Barbieri, R and Lo Giudice, M T *Z. Anorg. Allg. Chem.*, 1977, 432: 51
49. Preut, H, Mundus, B, Huber, F and Barbieri, R *Acta Cryst.*, 1986, C42: 536
50. Preut, H, Mundus, B, Huber, F and Barbieri, R *Acta Cryst.*, 1989, C45: 728
51. Vornfeld, M, Huber, F, Preut, H and von Angerer, E, *Appl. Organomet. Chem.*, in the press
52. Mundus-Glowacki, B, Huber, F, Preut, H, Ruisi, G and Barbieri, R *Appl. Organomet. Chem.*, 1992, 6: 83
53. Vornfeld, M, Huber, F, Preut, H, Ruisi, G and Barbieri, R *Appl. Organomet. Chem.*, 1992, 6: 75
54. Pellerito, L, Lo Giudice, M T, Ruisi, G, Bertrazzi, N, Barbieri, R and Huber, F *Inorg. Chim. Acta*, 1976, 17: L21
55. Barbieri, R, Pellerito, L and Huber, F *Inorg. Chim. Acta*, 1978, 30: L321
56. Huber, F and Ruisi, G unpublished results
57. David, S, Pascard, C and Cesario, M *Nouv. J. Chim.*, 1979, 3: 63
58. Holzapfel, C W, Koekemoer, J M, Marais, C F, Kruger, G J and Pretorius, J A S. *J. Chem.*, 1982, 35: 81
59. Davies, A G, Price, A J, Dawes, H M and Hursthouse, M B *J. Chem. Soc., Dalton Trans*, 1986: 297
60. Pellerito, L, Ruisi, G, Barbieri, R and Lo Giudice, M T *Inorg. Chim. Acta*, 1977, 21: L33
61. Ruisi, G, Lo Giudice, M T and Pellerito, L *Inorg. Chim. Acta*, 1984, 93: 161
62. Fitzsimmons, B W, Seeley, N J and Smith, A W *Chem. Commun.*, 1968: 390
63. Ridenour, R E and Flagg, E E *J. Organomet. Chem.*, 1969, 16: 393
64. Tan, T H, Dalziel, J R, Yeats, P A, Sams, J R, Thompson, R C and Aubke, F *Can. J. Chem.*, 1972, 50: 1843
65. Chivers, T, van Roode, J H G, Ruddick, J N R and Sams, J R *Can. J. Chem.*, 1973, 51: 3702
66. Denicke, K, Schmitt, R, Shihada, A F and Pebler, J Z. *Anorg. Allg. Chem.*, 1974, 404: 249
67. Cunningham, D, Kelly, L A, Molloy, K C and Zuckerman, J J *Inorg. Chem.*, 1982, 21: 1416
68. Molloy, K C, Nasser, F A K and Zuckerman, J J *Inorg. Chem.*, 1982, 21: 1711
69. Barbieri, R, Alonzo, G and Herber, R H *J. Chem. Soc., Dalton Trans*, 1987: 789
70. Chivers, T, van Roode, J H G, Ruddick, J N R and Sams, J R *Can. J. Chem.*, 1976, 54: 2184
71. Molloy, K C, Hossain, M B, van der Helm, D, Cunningham, D and Zuckerman, J J *Inorg. Chem.*, 1981, 20: 2402; Molloy, K C and Quill, K J. *Chem. Soc., Dalton Trans*, 1985: 1417
72. Blunden, S J, Hill, R and Gillies, D G *J. Organomet. Chem.*, 1984, 270: 39
73. May, L, Eng, G, Coddington, S P and Stockton, L L *Hyperfine Interact.*, 1988, 42: 909
74. Rabenstein, D L, Backs, S J and Isab, A A *J. Am. Chem. Soc.*, 1981, 103: 2836
75. Barbieri, R, Silvestri, A and Huber, F *Appl. Organomet. Chem.*, 1988, 2: 457
76. Barbieri, R, Silvestri, A, Filippeschi, S, Magistrelli, M and Huber, F *Inorg. Chim. Acta*, 1990, 177: 141
77. Silvestri, A, Duca, D and Huber, F *Appl. Organomet. Chem.*, 1988, 2: 417
78. Barbieri, R, Silvestri, A and Huber, F *Appl. Organomet. Chem.*, 1988, 2: 525
79. Stapfer, C H and Herber, R H, *J. Organomet. Chem.*, 1973, 56: 175
80. Smith, P J, Hyams, R L, Brooks, J S and Clarkson, R W, *J. Organomet. Chem.*, 1979, 171: C29
81. Domazetis, G, Magee, R J and James, B D, *J. Organomet. Chem.*, 1979, 173: 357

82. Cashion, J D, Domazetis, G and James, B D *J. Organomet. Chem.*, 1980, 185: 433
83. Bamgboye, O A, Bamgboye, T T and Harrison, P G *J. Organomet. Chem.*, 1986, 306: 17
84. Poller, R C and Ruddick, J N R, *J. Chem. Soc., Dalton Trans*, 1972: 555
85. Nesmeyanov, A N, Gol'danskii, V I, Khrapov, V V, Rochev, V Ya, Kravtsov, D N and Rokhlina, E M *Izv. Akad. Nauk SSSR, Ser. Khim.*, 1968: 793; Engl. Transl., p 763
86. Aldridge, W N, Street, B W and Noltes, J G *Chem.-Biol. Interact.*, 1981, 34: 223
87. Muetterties, E L and Schunn, R A, *Quart. Rev., Chem. Soc. (London)*, 1966, 20: 245
88. Bluhm, M M, Bodo, G, Dintzis, H M and Kendrew, J C *Proc. Roy. Soc.*, 1958, A246: 369
89. Blacke, C C F, *Adv. Protein Chem.*, 1968, 23: 59
90. Perutz, M F, Fermi, G, Abraham, D J, Poyart, C and Bursaux, E *J. Am. Chem. Soc.*, 1986, 108: 1064
91. Barbieri, R *Giornale di Fisica*, 1982, 23: 289
92. Yasuda, M and Tobias, R S *Inorg. Chem.*, 1963, 2: 207
93. Hynes, M J and O'Dowd, M J *Chem. Soc., Dalton Trans*, 1987: 563
94. Henninghausen, G and Merkord, J *Arch. Toxicol.*, 1985 57: 67
95. Huber, F, Roge, G, Carl, L, Atassi, G, Spreafico, F, Filippeschi, S, Barbieri, R, Silvestri, A, Rivarola, E, Ruisi, G, Di Bianca, F and Alonzo, G *J. Chem. Soc., Dalton Trans*, 1985: 523